verging into the Venus wake. Eventually the field strength decreases to very low values, but it increases later to quite large values near periapsis. Generally these field values are horizontal and do not appear rooted in the planet except in the region closest to the center of the wake. Outbound at higher altitudes the field is no longer horizontal at the same values of SZA as it was when the spacecraft was inbound; this result suggests that in this region the flow is not horizontal but more tailward away from the planet. Farther along the outbound leg the field reverses and becomes quite strong. The direction of the field in this display then follows the pattern of the inbound leg but reversed in direction. This pattern would be expected if the external field direction remained constant during the satellite's passage through the wake and these field lines were draped over the ionosphere. The opposite field directions seen in the center of the wake are therefore probably the remnants of some earlier magnetosheath field which had penetrated the ionosphere and been convected to the nightside, possibly in the form of flux ropes.

Figure 4 shows a similar display for orbit 72 during which the spacecraft penetrates closer to the wake axis than on orbit 66. Well away from the wake on both inbound and outbound passes the field directions suggest draping. Closer to the wake the pattern of the field vectors again suggests convergence of the flow into the night ionosphere. In the magnetic field there is no clear boundary between magnetosheath and ionospheric plasmas. However, there are distinct regions with different directions of magnetization. The existence of these differing field directions within the wake suggests that the field here is a remnant induced by earlier solar wind conditions. When the data for entire orbits become available, we will be able to determine when this field direction was impressed on the ionosphere.

Although there are strong magnetic fields on the nightside of Venus, there is little evidence that these fields arise from an internal dynamo. A Venus magnetic moment of 10^{22} gauss-cm^3 would give rise to a 10-nT polar field. If such a field were present, it would certainly be evident in displays such as Figs. 3 and 4. Instead, the field is mainly horizontal near the planet. Furthermore, the direction of the field in the wake on these orbits is opposite to that seen on the Mariner 5 and Venera 4 missions (*5*, *6*). A firm upper limit to the moment awaits a comprehensive study of all the nightside data, but it would certainly seem at this stage that such a limit will be much less than 10^{22} gauss-cm^3. The rapid convergence of the field toward the wake axis implies slow flows into the wake at low altitudes. The direction of the large fields near periapsis often differs from what we would expect, given the direction of the field outside of the ionosphere. Thus, these low-altitude wake fields appear to be remnants of some previously induced current. It seems improbable, because of their variability from orbit to orbit, that they are intrinsic fields.

Prior to the Pioneer Venus measurements, the Venus magnetic field appeared to be surprisingly weak. These measurements increase the gap between expectation and observation. It is most likely that at present Venus does not have an active magnetic dynamo. Since Venus rotates and most certainly has a liquid conducting core, the explanation probably lies in the fact that the magnetic Reynold's number is not high enough for dynamo action. This fact in turn suggests simply that the convective motion in the interior of Venus is not strong enough to generate a field. Weak convective motion could be due either to the present state of thermal evolution of Venus or to some chemical or physical difference between the interiors of Venus and Earth.

C. T. Russell
R. C. Elphic, J. A. Slavin
Institute of Geophysics and Planetary Physics, University of California, Los Angeles 90024

References and Notes

1. J. A. Jacobs, *Geophys. Res. Lett.* **6**, 213 (1979).
2. F. H. Busse, *Phys. Earth Planet. Interiors* **12**, 350 (1976).
3. C. T. Russell, R. C. Elphic, J. A. Slavin, *Science* **203**, 745 (1979).
4. For further details on the instrumentation, see R. C. Snare and J. D. Means, *IEEE Trans. Magn.* **MAG-13**, 1107 (1977).
5. H. S. Bridge, A. J. Lazarus, C. W. Snyder, E. J. Smith, L. Davis, Jr., P. J. Coleman, Jr., D. E. Jones, *Science* **158**, 1669 (1967); C. T. Russell, *Geophys. Res. Lett.* **3**, 589 (1976).
6. Sh. Sh. Dolginov, Ye. G. Yeroshenko, L. Davis, *Kosm. Issled.* **7**, 747 (1969).
7. C. T. Russell, *Geophys. Res. Lett.* **3**, 125 (1976).
8. Sh. Sh. Dolginov, L. N. Zhuzgov, V. A. Sharova, V. B. Buzin, Ye. G. Yeroshenko, "Magnetosphere of the planet Venus" (in Russian) (IZMIRAN preprint 19, Moscow, 1977).
9. Times used are universal times at Venus.
10. This work was carried out under NASA contract NAS2-9491. Contribution No. 1922 of the Institute of Geophysics and Planetary Physics, University of California at Los Angeles.

15 May 1979

Electron Observations and Ion Flows from the Pioneer Venus Orbiter Plasma Analyzer Experiment

Abstract. *Additional plasma measurements in the vicinity of Venus are presented which show that (i) there are three distinct plasma electron populations—solar wind electrons, ionosheath electrons, and nightside ionosphere electrons; (ii) the plasma ion flow pattern in the ionosheath is consistent with deflected flow around a blunt obstacle; (iii) the plasma ion flow velocities near the downstream wake may, at times, be consistent with the deflection of plasma into the tail, closing the solar wind cavity downstream from Venus at a relatively close distance (within 5 Venus radii) to the planet; (iv) there is a separation between the inner boundary of the downstream ionosheath and the upper boundary of the nightside ionosphere; and (v) during the first 4.5 months in orbit the measured solar wind plasma speed continued to vary, showing a number of high-speed, but generally nonrecurrent, streams.*

In this report we present additional (*1*) early results from the Pioneer Venus orbiter plasma analyzer experiment. Most of these results are based on the available real-time data. Least-squares reduction of the few data tapes we have received provided the ion flow velocities.

Our early Pioneer Venus observations (*1*) indicated that the solar wind interaction at Venus is dynamic and consistent with a solar wind ionosphere-atmosphere interaction. Recently, Intriligator and Smith (*2*) calculated that the atmospheric-ionospheric particle pressure at Venus [as measured by the Pioneer Venus orbiter experiments (*3*)] is sufficient to hold off the external solar wind. The implied primarily nonmagnetic planetary solar wind interaction is consistent with Pioneer Venus magnetic field measurements (*4*) and unlike the interactions at Earth or Jupiter.

In this report we further explore this interaction by presenting preliminary plasma electron and ion observations in the ionosheath and in the vicinity of the wake. Finally, since the solar wind–Venus interaction is very dynamic and since the configuration of the Venus ionosphere, on the sunward side at least, appears to be coupled to the external solar wind (*1*, *3*), we present the daily solar wind speeds from orbit insertion (4 December 1978) through 18 April 1979.

0036-8075/79/0706-0116$00.50/0

Plasma electron observations. As indicated in Wolfe *et al.* (*1*), our initial electron observations indicate that the plasma electron parameters appear to be consistent with those of the plasma ions. In this report Figs. 1 and 2 are our initial presentation of observations of plasma electrons in the vicinity of Venus. All energy-dependent corrections have been made, so Figs. 1 and 2 show the measured relative differential electron current as a function of energy, measured in two instrument modes, covering two adjacent energy ranges, running from nearly 0 to 250 eV. The top panels in Fig. 1 show a typical solar wind electron spectrum. The middle panels, a typical ionosheath spectrum, show a broader peak in the higher energies, most likely associated with thermal heating of solar wind electrons across the Venus bow shock. The peak at lowest energies, on the left in both the solar wind and the ionosheath spectra, is identified as primarily associated with photoelectrons from the spacecraft. The bottom panels show a typical nightside ionosphere electron spectrum, recorded in the optical shadow of Venus and lacking a low-energy peak, consistent with the association of the low-energy peak with spacecraft photoelectrons.

Since tapes are not yet available for data obtained in the vicinity of Venus and in the solar wind, it is not possible at this time to present plasma electron densities and more detailed plasma electron parameters. It is anticipated that these parameters will be published once the data tapes have been received and processed.

Figure 2 is a series of successive electron energy spectra on 21 February 1979. The spectra at 2008 and 2014 universal time (UT) were obtained in the nightside ionosphere when the spacecraft was in optical shadow; thus the lower-energy spectra (on the left) show the absence of a photoelectron peak. An expanded vertical scale for the higher-energy spectra indicates the presence of enhanced current levels for these same times (2008 and 2014 UT). The absence of a photoelectron peak and the enhanced current levels at the higher energies in the nightside ionosphere are discussed later with regard to the maintenance of the nightside ionosphere.

The next three sets of electron energy spectra (2019, 2025, and 2030 UT) were obtained in the ionosheath. The lower-energy portions of these spectra show the prominent peak associated primarily with photoelectrons after the reemergence of the spacecraft into the sunlight. The higher-energy portions show the thermalization of solar wind electrons across the bow shock. Note the particularly broad and large (that is, hot and dense) distribution at 2030 UT, just inside the bow shock. The subsequent spectra were obtained later in the outbound portion of the orbit and the final spectrum, obtained at 2046 UT, indicates the reemergence of the spacecraft into the free-stream solar wind.

Plasma ion observations. Preliminary determination of the Venus ionosheath flow field is shown in Figs. 3 and 4. These are the results obtained from orbits 3, 5, 6, 72, 74, and 77. This particular choice of orbits was dictated by the availability of data tapes and was not made for any illustrative purpose. The flow field is therefore incomplete at this time. Nevertheless, it is clear in Fig. 3, which gives a projection into the noon-midnight meridian plane of unaberrated ionosheath proton flow velocity vectors, that the flow pattern is consistent with postshock solar wind flow around the blunt-obstacle shape of the dayside ionopause. The unaberrated proton velocity vectors projected on the Venus orbital plane (viewed from the north) in Fig. 4 show a relatively small deflection compared to that in Fig. 3; this is because the locations where the flow was observed were not far from the sun-Venus line in this projection. Even here, however, a pattern consistent with postshock flow is evident.

On the meridian plane plot of Fig. 3,

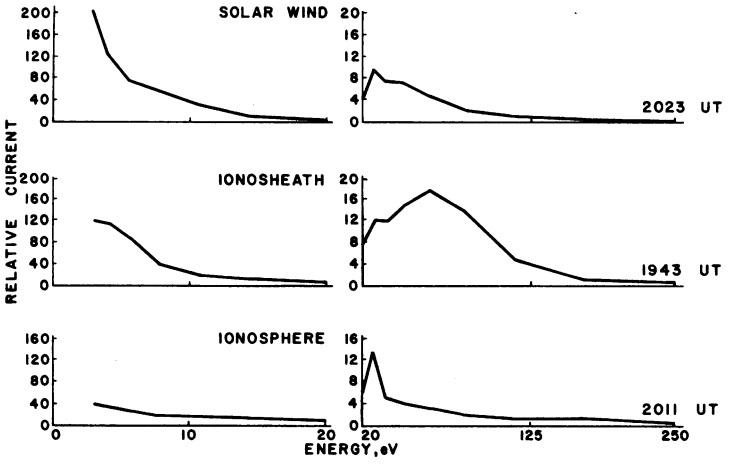

Fig. 1 (left). Comparison of typical plasma differential electron energy spectra, corrected for energy-dependent instrumental effects, from the solar wind, the ionosheath, and the nightside ionosphere. The lower-energy (mode 1) spectra are shown on the left and the higher-energy (mode 2) spectra on the right. Fig. 2 (right). Successive electron spectra as in Fig. 1, near periapsis on 21 February 1979, showing the change in spectral characteristics as the spacecraft passes from the nightside ionosphere (2008 and 2014 UT), through the ionosheath (2019, 2025, and 2030 UT), and into the solar wind (2046 UT). Exact times of the boundaries between these three regions have not been determined yet. The highest energies of the nightside ionosphere spectra in Figs. 1 and 2 and other data show evidence of current levels enhanced over backgrounds estimated from solar wind measurements.

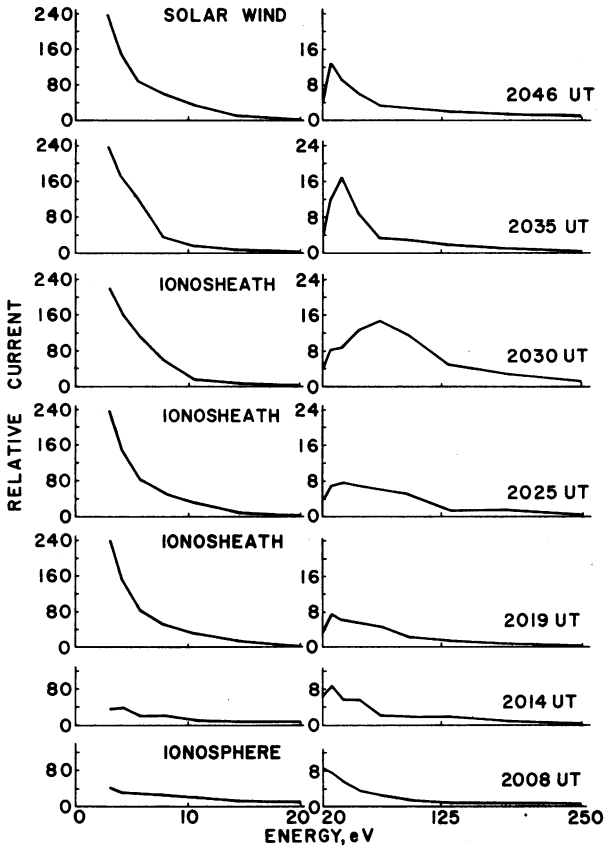

solid bars show where deflections of ionosheath plasma flow toward the Venus solar wind cavity were observed in the real-time data for 11 orbits between orbits 36 and 95. Deflection here means a shift of the peak plasma flux out of the central collector of the five in the instrument corresponding to a flow deflection of approximately 15°. These are the only cases found in real-time data through orbit 114. The deflections toward the cavity occur at various proton energies, appear sporadic in time, and are all observed well outside the Venus optical shadow. Flow deflections of approximately 10° to 15° imply that some ionosheath plasma should occasionally be detected throughout the region of the Venus optical shadow beginning approximately 4 to 7 Venus radii (R_V) downstream from the planet. Alternatively, these deflections may be associated with changes in the interplanetary solar wind flow direction or local plasma instabilities, which would give rise to tail or cavity oscillations with actual tail closure being much farther downstream. Because of the incomplete nature of the data, it is not possible to choose between these alternatives (or possibly others) at this time.

Daily values of the peak speed of the solar wind protons, obtained from Venus orbit insertion (4 December 1978) through orbit 135 on 18 April 1979, are given in Fig. 5. These solar wind speeds were taken from the real-time data at approximately noon UT on each day and represent interplanetary values several hours upstream from the bow shock on the inbound leg of each orbital pass.

There are numerous high-speed streams evident in the data, with peak speeds ranging from about 400 to 750 km/sec and the quiescent solar wind speed generally near 300 km/sec. It is clear, however, that there is no strong tendency for the stream structure to show recurrence with respect to the synodic rotational period of the sun (28.0 days). This is most likely due to coronal temporal variations typical of the rising portion of the solar cycle near solar maximum (*5*).

Discussion. Although most of the data are very preliminary, we are able to reach several interesting conclusions regarding the nature of the solar wind interactions at Venus.

The electron observations show possibly enhanced current levels in the nightside ionosphere (Figs. 1 and 2); these may be associated with physical processes connected with the maintenance and energetics of the nightside ionosphere (*6*, *7*), the location of the nightside ionopause (*8*), and the other nightside ionospheric phenomena.

To calculate the ionization rate due to electrons in the energy range 0.05 to 0.25 keV, we used a modified version of the program previously employed for computing photoelectron fluxes (*9*). Measurements on orbit 57 showed enhanced electron current between 50 and 250 eV although no angular distribution for these energies was available in the data at that time. We assumed an isotropic distribution, made a preliminary estimate for the downward electron flux of 5×10^{-7} cm^{-2} sec^{-1}, and inserted this flux into the existing model as the upper boundary condition for the most energetic bin at 70 eV. The computed ionization rate at an altitude of 150 km was ~15 electron-ion pairs per cubic centimeter per second, with values decreasing rapidly with increasing altitude. The CO_2^+ ions so formed rapidly undergo reaction with O to produce O_2^+. For the observed electron temperature (*10*) (~1000 K) at 150 km, the dissociative recombination coefficient (*11*) is about 8×10^{-8} cm^3 sec^{-1}, leading to a predicted O_2^+ number density of (1 to 2) $\times 10^4$ cm^{-3}. This O_2^+ concentration is of the same order as the average observed (*12*) and inferred (*7*, *13*) values at an altitude of ~150 km on several orbits. Thus we conclude that our observed electron fluxes below the nightside ionopause may be sufficient to account for the observed O_2^+ density at ~150 km altitude. As indicated above, the production of these ions is consistent with the results from other Pioneer Venus experiments.

It should be noted that for the sunward hemisphere the boundary defined by the exclusion of the postshock solar wind ionosheath flow is coincident with the upper boundary of the ionosphere and has been called the ionopause (*1*, *3*). However, downstream from the terminator, inspection of the real-time data

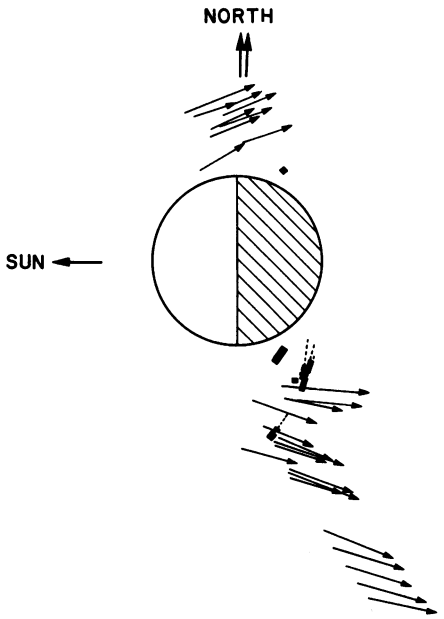

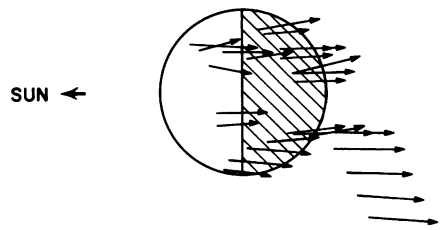

Fig. 3 (left). Unaberrated ionosheath proton velocity vectors measured on orbits 3, 5, 6, 72, 74, and 77, projected into the noon-midnight meridian plane. The change during this time of the direction toward the north, due to the slight inclination of Venus' orbit to the ecliptic, is indicated. Solid bars indicate the locations where inward deflection (toward the antisolar line) was observed in the real-time data. The dashes associated with some of the solid bars indicate missing real-time data (to be available later) so that slow deflections could not be determined. Fig. 4 (right). Similar to Fig. 3 but projected on the Venus orbital plane.

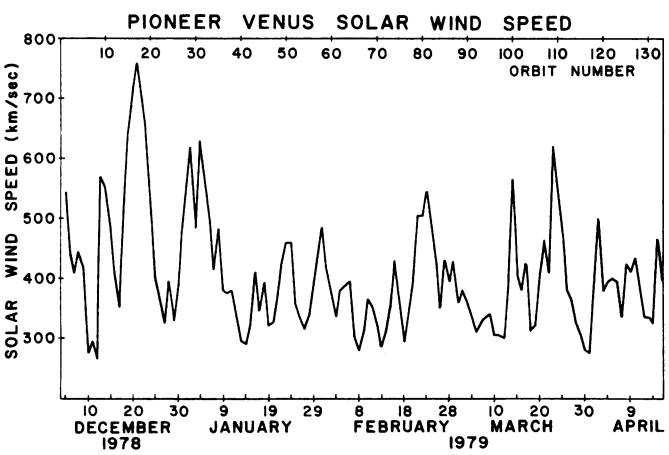

Fig. 5. Daily solar wind peak speeds measured for each of the first 135 orbits. Values were obtained near noon UT for each orbit, upstream from the bow shock.

shows a cessation of ionosheath flow at radial distances greater than those reported for the ionospheric boundary (*8*). The separation of these two boundaries becomes progressively larger as the sun-Venus-spacecraft angle increases beyond the terminator. This indicates the presence of a cavity on the nightside defined on one side by the inner boundary of the ionosheath and on the other side by the outer boundary of the ionosphere. The inward flow deflections observed thus far, as discussed in connection with Fig. 3, indicate that this cavity is cone-shaped with the cavity closure at times perhaps as close to the planet as about 5 R_V. This result is consistent with the Venera 9 and Venera 10 measurements by Vaisberg *et al.* (*14*) and with other work (*15*).

D. S. INTRILIGATOR
Physics Department,
University of Southern California,
Los Angeles 90007

H. R. COLLARD
J. D. MIHALOV
R. C. WHITTEN
J. H. WOLFE
Space Science Division,
NASA Ames Research Center,
Moffett Field, California 94035

References and Notes

1. J. Wolfe, D. S. Intriligator, J. Mihalov, H. Collard, D. McKibbin, R. Whitten, A. Barnes, *Science* **203**, 750 (1979).
2. D. S. Intriligator and E. J. Smith, in preparation.
3. L. H. Brace, R. F. Theis, J. P. Krehbiel, A. F. Nagy, T. M. Donahue, M. B. McElroy, A. Pedersen, *Science* **203**, 763 (1979); H. A. Taylor, Jr., *et al.*, *ibid.*, p. 755.
4. C. T. Russell, R. C. Elphic, J. A. Slavin, *ibid.*, p. 745.
5. D. S. Intriligator, *Astrophys. J.* **221**, 1009 (1978).
6. K. I. Gringauz, M. I. Verigin, T. K. Breus, T. Gombosi, *J. Geophys. Res.* **84**, 2123 (1979); R. H. Chen and A. F. Nagy, *ibid.* **83**, 133 (1978); H. Perez de Tejada, *Geofis. Int.*, in press.
7. A. J. Kliore, I. R. Patel, A. F. Nagy, T. E. Cravens, T. I. Gombosi, *Science* **205**, 99 (1979).
8. L. H. Brace, H. A. Taylor, Jr., P. A. Cloutier, R. E. Daniell, Jr., A. F. Nagy, *Geophys. Res. Lett.* **6**, 345 (1979).
9. P. T. McCormick, P. F. Michelson, D. W. Pettibone, R. C. Whitten, *J. Geophys. Res.* **81**, 5196 (1976).
10. W. C. Knudsen, K. Spenner, R. C. Whitten, J. R. Spreiter, K. L. Miller, V. Novak, *Science* **205**, 105 (1979).
11. P. M. Banks and G. Kockarts, *Aeronomy* (Academic Press, New York, 1973), part A, pp. 255–256.
12. W. C. Knudsen, private communication; H. A. Taylor, Jr., H. C. Brinton, S. J. Bauer, R. C. Hartle, P. A. Cloutier, R. E. Daniell, Jr., T. M. Donahue, *Science* **205**, 96 (1979).
13. L. H. Brace, R. F. Theis, H. B. Niemann, H. G. Mayr, W. R. Hoegy, A. F. Nagy, *Science* **205**, 102 (1979).
14. O. L. Vaisberg, S. A. Romanov, V. N. Smirnov, I. P. Karpinsky, B. I. Khazanov, B. V. Polenov, A. V. Bogdanov, N. M. Antonov, in *Physics of Solar Planetary Environments*, D. J. Williams, Ed. (American Geophysical Union, Washington, D.C., 1976), p. 904.
15. H. Perez de Tejada and M. Dryer, *J. Geophys. Res.* **81**, 2023 (1976).
16. Supported in part by NASA contract NAS2-9478 and by the University of Southern California.

15 May 1979

Gamma-Ray Burst Observations by Pioneer Venus Orbiter

Abstract. *The Pioneer Venus orbiter gamma burst detector is an astrophysics experiment for monitoring cosmic gamma-ray bursts. It is included in this planetary mission to provide a long baseline for accurately locating the sources of these bursts in order to identify them with specific astronomical objects. Responses to 14 gamma-ray burst events were examined; these events were verified from data acquired by other systems. Preliminary locations are proposed for three events, based on data from the Pioneer Venus orbiter, ISEE C, and Vela spacecraft. These locations will be improved, and additional locations will be determined by including in the analyses data from Helios B and the Russian Venera 11, Venera 12, and Prognoz 7 spacecraft.*

The orbiter gamma burst detector (OGBD) was placed in service about 1 day after the launch of the Pioneer Venus orbiter spacecraft. The instrument thereupon functioned continuously until it was turned off in preparation for orbital injection. After orbital injection the instrument was turned back on, and it has provided continuous observations through the time of this writing.

The OGBD is not truly a participant in the investigations of the planet Venus, but was included to perform astrophysical observations from a platform far removed from Earth. Early in our considerations of the gamma-ray burst (GRB) phenomenon, it became apparent that the identification of GRB sources with other known astronomical objects was of major importance for understanding the mechanisms of generation of these bursts. Since these events occur infrequently and unpredictably, an instrument capable of independently locating the source of each burst with reasonable accuracy and efficiency would need to be massive and complex. Consequently, it was decided to extend the simple locating technique that has been employed with the Vela data (*1*), namely that of triangulation between multiple observing platforms, using time-of-arrival differences between the widely distributed array elements. Clearly, the precision in this technique of location could be improved by simply increasing the separation between members of the array. It was on this basis that the OGBD, which is a modest instrument by the standards of gamma-ray astronomy, was proposed to be included among the complement of the Pioneer Venus orbiter spacecraft.

The OGBD consists of two sensor

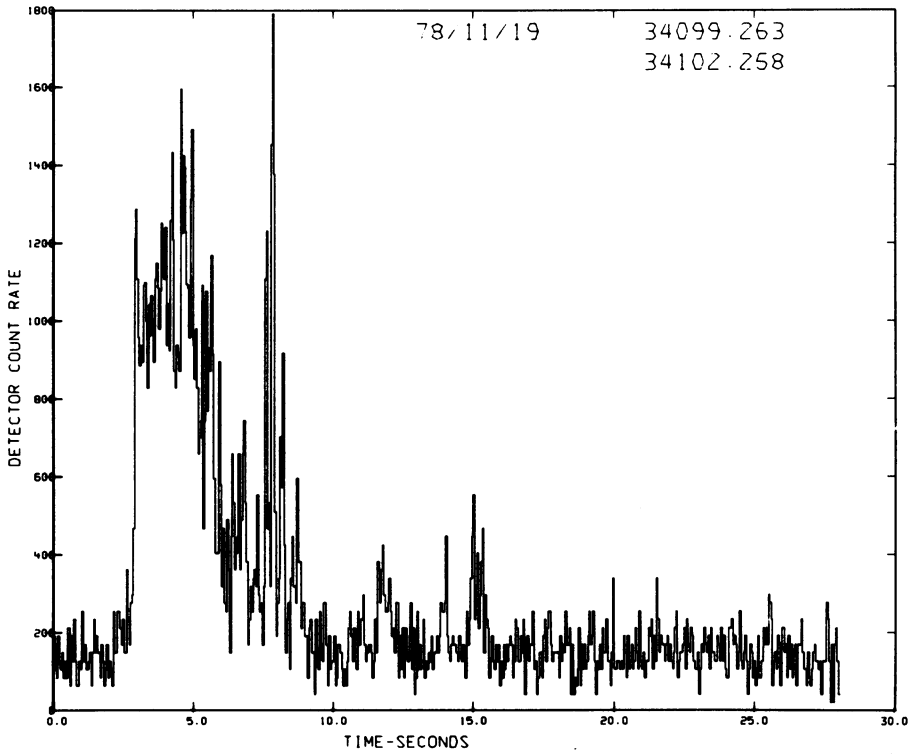

Fig. 1. Event record of 19 November 1978, illustrating the time structure of the count rate in the full energy channel (0.1 to 2.0 MeV) and displaying the entire contents of the experiment memory.

0036-8075/79/0706-0119$00.50/0